Search for a Dark Photon in Electro-Produced e^+e^- Pairs with the Heavy Photon Search Experiment at JLab

P. Hansson Adrian,[1] N.A. Baltzell,[2] M. Battaglieri,[3] M. Bondí,[4] S. Boyarinov,[2] S. Bueltmann,[5] V.D. Burkert,[2] D. Calvo,[6] M. Carpinelli,[7] A. Celentano,[3] G. Charles,[5] L. Colaneri,[8] W. Cooper,[9] C. Cuevas,[2] A. D'Angelo,[8] N. Dashyan,[10] M. De Napoli,[4] R. De Vita,[3] A. Deur,[2] R. Dupre,[11] H. Egiyan,[2] L. Elouadrhiri,[2] R. Essig,[12] V. Fadeyev,[13] C. Field,[1] A. Filippi,[6] A Freyberger,[2] M. Garçon,[14] N. Gevoryan,[10] F.X. Girod,[2] N. Graf,[1] M. Graham,[1] K.A. Griffioen,[15] A. Grillo,[13] M. Guidal,[11] R. Herbst,[1] M. Holtrop,[16] J. Jaros,[1] G. Kalicy,[5] M Kahndaker,[17] V. Kubarovsky,[2] E. Leonora,[4] K. Livingston,[18] T. Maruyama,[1] K. McCarty,[16] J. McCormick,[1] B. McKinnon,[18] K. Moffeit,[18] O. Moreno,[1,13] C. Munoz Camacho,[11] T. Nelson,[1] S. Niccolai,[11] A. Odian,[1] M. Oriunno,[1] M. Osipenko,[3] R. Paremuzyan,[16] S. Paul,[15] N. Randazzo,[4] B. Raydo,[2] B. Reese,[1] A. Rizzo,[8] P. Schuster,[1,19] Y.G. Sharabian,[2] G. Simi,[20] A. Simonyan,[10] V. Sipala,[7] D. Sokhan,[18] S. Stepanyan,[2] N. Toro,[1,19] S. Uemura,[1] M. Ungaro,[2] H. Vance,[5] H. Voskanyan,[10] L.B. Weinstein,[5] B. Wojtsekhowski,[2] and B. Yale[16]

[1] *SLAC National Accelerator Laboratory, Stanford University, Stanford, CA 94309, USA*
[2] *Thomas Jefferson National Accelerator Facility, Newport News, Virginia 23606*
[3] *INFN, Sezione di Genova, 16146 Genova, Italy*
[4] *Istituto Nazionale di Fisica Nucleare, Sezione di Catania e Dipartimento di Fisica dell'Universit'a, Catania, Italy*
[5] *Old Dominion University, Norfolk, Virginia 23529*
[6] *INFN, Sezione di Torino, 10125 Torino, Italy*
[7] *Universit'a di Sassari, 07100 Sassari, Italy*
[8] *Universit'a di Roma Tor Vergata, 00133 Rome Italy*
[9] *Fermi National Accelerator Laboratory, Main Entrance Rd, Batavia (IL), USA*
[10] *Yerevan Physics Institute, 375036 Yerevan, Armenia*
[11] *Institut de Physique Nucléaire, CNRS/IN2P3 and Université Paris Sud, Orsay, France*
[12] *Department of Physics and Astronomy, Stony Brook University, Stony Brook, NY 11794, USA*
[13] *Santa Cruz Institute for Particle Physics, University of California, Santa Cruz, CA 95064, USA*
[14] *IRFU, CEA, Université Paris-Saclay, F-91191 Gif-sur-Yvette, France*
[15] *College of William and Mary, Williamsburg, Virginia 23187-8795*
[16] *University of New Hampshire, Durham, New Hampshire 03824-3568*
[17] *Norfolk State University, Norfolk, Virginia 23504*
[18] *University of Glasgow, Glasgow G12 8QQ, United Kingdom*
[19] *Perimeter Institute, Ontario, Canada N2L 2Y5*
[20] *Universit'a degli di Padova, 35122 Padova, Italy*

(Dated: July 18, 2018)

The Heavy Photon Search experiment took its first data in a 2015 engineering run at the Thomas Jefferson National Accelerator Facility, searching for a prompt, electro-produced dark photon with a mass between 19 and 81 MeV/c^2. A search for a resonance in the e^+e^- invariant mass distribution, using 1.7 days (1170 nb^{-1}) of data, showed no evidence of dark photon decays above the large QED background, confirming earlier searches and demonstrating the full functionality of the experiment. Upper limits on the square of the coupling of the dark photon to the Standard Model photon are set at the level of 6×10^{-6}. Future runs with higher luminosity will explore new territory.

PACS numbers:

I. INTRODUCTION

The search for low-mass hidden sectors weakly coupled to the Standard Model (SM) has received increased attention over the last decade [1**?** –4]. Hidden sectors are motivated by the existence of dark matter, appear in myriad extensions of the SM, and have been invoked to explain a wide variety of experimental anomalies.

A prototypical hidden sector consists of a spontaneously broken "hidden" $U(1)'$ gauge symmetry, whose mediator is the "heavy photon" or "dark photon", A'. The heavy photon interacts with SM particles through kinetic mixing with the $U(1)_Y$ (hypercharge) gauge boson [5, 6], resulting in the effective lagrangian density

$$\mathcal{L} \supset -\frac{\epsilon}{2\cos\theta_W} F'_{\mu\nu} F_Y^{\mu\nu} \,. \tag{1}$$

Here ϵ is the kinetic-mixing parameter, θ_W is the Weinberg mixing angle, $F'_{\mu\nu} = \partial_\mu A'_\nu - \partial_\nu A'_\mu$ is the $U(1)'$ field strength, and similarly $F_Y^{\mu\nu}$ denotes the SM hypercharge $U(1)_Y$ field strength. This mixing generates an interaction between the A' and the SM photon at low energies, allowing dark photons to be produced in charged particle interactions and, if sufficiently massive, to decay into pairs of charged particles like e^+e^- or hidden-sector states. The value of ϵ is undetermined, but a value of $\epsilon^2 \sim 10^{-8} - 10^{-4}$ is natural if generated by quantum effects of heavier particles charged under $U(1)'$ and $U(1)_Y$.

If the SM forces unify in a Grand Unified Theory, then $\epsilon^2 \sim 10^{-12} - 10^{-6}$ is natural [7–9]. The mass of the A', $m_{A'}$, is also undetermined, but the MeV-to-GeV mass scale has received much attention over the last decade as a possible explanation for various anomalies related to dark matter interacting through the A' [10–14] and for the discrepancy between the observed and SM value of the muon anomalous magnetic moment [15–17]. Moreover, this mass range appears naturally in a few specific models [7–9, 18, 19].

The Heavy Photon Search (HPS) is an experiment utilizing the CEBAF accelerator at the Thomas Jefferson National Accelerator Facility (JLab) in Newport News, Virginia, USA. The experiment can explore a wide range of masses ($m_{A'} \sim 20 - 500$ MeV/c^2) and couplings ($\epsilon^2 \sim 10^{-6} - 10^{-10}$), using both resonance search and separated vertex strategies. In this paper, results of a resonance search from a Spring 2015 engineering run using a 50 nA, 1.056 GeV electron beam impinging on a thin ($0.125\%X_0$) tungsten target are reported. Electron interactions with the target nuclei could produce an A' particle, which could subsequently decay to an e^+e^- pair [20–22]. A spectrometer, triggered by an electromagnetic calorimeter, measures the momenta and trajectories of this pair, allowing for the reconstruction of its invariant mass and decay position. The A' would appear as a narrow resonance, with a width set by the mass resolution, on top of a smooth and wide distribution of background events from ordinary quantum electrodynamic (QED) processes.

The cross section for A' production and subsequent decay to e^+e^- ("radiative A' production") scales with ϵ^2 and is directly proportional to the cross section for e^+e^- pair production from virtual photon bremsstrahlung ("radiative trident production") [20], so their yields are proportional. We assume the A' only decays to e^+e^-, as expected below the di-muon threshold if there are no invisible A' decays. The measured e^+e^- yield, $dN/dm_{A'}$, is accounted for by the sum of trident and wide-angle bremsstrahlung (WAB) processes. Both radiative and Bethe Heitler diagrams contribute to trident production. WABs contribute if the photon converts and the resulting positron is detected along with the electron which has radiated. After accounting for the converted WABs, the trident yield is known. The fraction of all tridents which are radiative can be calculated, so the radiative trident yield is also determined, fixing the sensitivity of the search. The experimental mass resolution impacts the experimental reach and is a critical input to the fits of the mass spectrum; it is calibrated by measuring the invariant mass of Møller pairs, which have a unique invariant mass for any given incident electron energy.

The outline of the rest of the paper is as follows. In Sec. II, we describe the experimental setup and the detector. Sec. III discusses the selection of the events to maximize the A' signal over the QED background. Sec. IV describes the analysis of the resonance search, while Sec. V presents the results. Our conclusions are presented in Sec. VI.

II. DETECTOR OVERVIEW

The kinematics of A' electro-production result in very forward-produced heavy photons, which carry most of the beam energy and decay to highly-boosted e^+e^- pairs. To accept these decays, the HPS detector is designed as a compact forward magnetic spectrometer, consisting of a silicon vertex tracker (SVT) placed in a vertical dipole magnetic field for momentum measurement and vertexing, and a $PbWO_4$ crystal electromagnetic calorimeter (ECal) for event timing and triggering. The SVT consists of six layers of detectors located in vacuum between 10 and 90 cm from the target, and arranged just above and below the "dead zone", a horizontal fan of intense flux from beam particles which have scattered or radiated in the target. Each layer consists of two silicon microstrip sensors with a small (50 or 100 mrad) stereo angle for three dimensional position determination [23]. The ECal has 442 crystals and is situated downstream of the tracker [24]. The ECal is split above and below the vacuum chamber which transports the beam towards the dump.

HPS searches for a small signal above the much larger QED trident background, so it must accumulate high statistics. This was accomplished using CEBAF's nearly continuous beam, SVT and ECal readout with precision timing, and a high rate data acquisition system. The CEBAF accelerator provided a very stable beam with negligible halo, focused to a $\sim$100 μm spot at the target [25]. The SVT was read out using the APV25 ASIC operating at 40 MHz [26] and triggered data from each sensor was sent to the SLAC ATCA-RCE readout system [27]. The ECal was read out with a 250 MHz JLab FADC [28]. A custom trigger used the ECal information to select events consistent with coming from a high-energy e^+e^- pair. The data acquisition system could record events at rates up to 25 kHz with less than 15% deadtime.

The analyzing magnet provided a field of 0.25 Tesla. The resulting SVT momentum resolution is $\delta p/p = 7\%$ for beam energy electrons and is approximately constant for all momenta of interest [23]. The ECal has an energy resolution $\delta E/E = 5.7\%$ at 0.5 GeV with significant energy and position dependence [24]. Using information from the ECal and the SVT, we select e^+e^- pairs and reconstruct their invariant mass and vertex positions. This gives the experiment access to two regions of parameter space, comparatively large couplings using a traditional resonance search strategy, and very small couplings using the distance from the target to the decay vertex to eliminate almost all of the prompt trident background.

The HPS detector was installed and commissioned within the Hall B alcove at JLab early in the spring of 2015 and subsequently took its first data. In total, 1170 nb^{-1} of data was collected (corresponding to 7.25 mC of integrated charge), equivalent to 1.7 days of continuous

running.

III. EVENT SELECTION

Searching for a heavy photon resonance requires accurate reconstruction of the e^+e^- invariant mass spectrum; rejection of background events due to converted WAB events, non-radiative tridents from the Bethe-Heitler process, and occasional accidental e^+e^- pairs; and efficient selection of A' candidates. Selecting A' candidates is equivalent to selecting radiative tridents since they have identical kinematics for a given mass. In order to perform a blind search, the event selection was optimized using ∼10% of the 2015 engineering run dataset.

Heavy photon candidates are created from pairs of electron and positron tracks, one in each half of the SVT, each of which point to an energy cluster in the ECal. Each track must pass loose quality requirements and have a reconstructed momentum less than 75% of the beam energy (0.788 GeV/c^2) to reject scattered beam electrons. The background from accidental pairs was reduced to less than 1% by requiring the time between the ECal clusters be less than 2 ns and the time between a track and the corresponding cluster be less than 5.8 ns.

Heavy photons decay to highly boosted e^+e^- pairs, while the recoiling electron is soft, scatters to large angles, and is usually undetected. Radiative tridents, having identical kinematics, comprise an irreducible background. The Bethe-Heitler diagram also contributes to trident production, and in fact dominates over the radiative process at all pair momenta. This background is minimized by requiring the momentum sum of the e^+e^- pair to be greater than 80% of the beam energy (0.84 GeV/c^2), where the radiative tridents are peaked.

The other significant source of background arises from converted WAB events in which the bremsstrahlung photon is emitted at a large angle (> 15 mrad), converts in the first or second layer of the SVT, and gives rise to a detected positron in the opposite half of the detector from the recoiling incoming electron. Although the fraction of such WAB events that convert with this topology is extremely low, it is offset by the fact that the bremsstrahlung rate is huge compared to the trident rate. This results in converted WAB events making up roughly 30% of our sample.

The converted WAB background was substantially reduced by applying additional selection criteria. Since the conversion usually happens in the first layers of the silicon detector, requiring both tracks to have hits in the first two layers of the SVT removes most of the converted WABs. Requiring the transverse momentum asymmetry between the electron and positron be $\frac{p_t(e^-)-p_t(e^+)}{p_t(e^-)+p_t(e^+)} < 0.47$ and the transverse distance of closest approach to the beam spot be less than 1.1 mm removes many of the remaining conversions. With all these cuts, contamination from converted WABs is reduced to 12%.

The composition of our event sample was checked by comparing the rates and distributions of several key variables (e.g total pair energy, electron energy, positron energy, and invariant mass) between data and Monte Carlo (which included tridents, converted WABs, and accidental background). We find that the data and MC are in reasonable agreement.

IV. RESONANCE SEARCH

A heavy photon will appear as a Gaussian-shaped resonance above the e^+e^- invariant mass spectrum, centered on the A' mass and with a width, $\sigma_{m_{A'}}$, which characterizes the experimental mass resolution. Møller scattering events ($e^-e^- \to e^-e^-$) are used to calibrate the A' mass scale and resolution. Figure 1 shows the measured Møller invariant mass, after a series of quality and selection cuts. For incident electrons of energy 1.056 GeV, we observe a Møller mass peak of 33.915 ± 0.043 MeV, within 1% agreement of the expected mass of 34.1 MeV. The Møller mass resolution predicted by Monte Carlo is 1.30 ± 0.02 MeV, in contrast with the observed value of 1.61 ± 0.04 MeV. We ascribe the difference to the fact that our measured momentum resolution for beam energy electrons (7.03%) is significantly worse than predicted by Monte Carlo (5.9%). Since the mass resolution scales directly with the momentum resolution, it is underestimated in Monte Carlo by 19%. Consequently, we scale up the simulated A' mass resolution by a factor of 1.19. The resulting parameterization of the mass resolution is an input to the resonance search.

Since the mass of a putative A' is unknown a priori, the entire e^+e^- invariant mass spectrum is scanned for any significant peaks. This search is performed in a broad mass window around each candidate mass, repeated in 0.5 MeV steps across the entire spectrum. Within the window, which is $14\sigma_{A'}$ wide below 39 MeV and $13\sigma_{A'}$ wide between 39 and 81 MeV, the invariant mass distribution of e^+e^- events is modeled using the probability distribution function

$$P(m_{e^+e^-}) = \mu \cdot \phi(m_{e^+e^-}|m_{A'}, \sigma_{m_{A'}}) + B \cdot \exp(p(m_{e^+e^-}|\mathbf{t})) \quad (2)$$

where $m_{e^+e^-}$ is the e^+e^- invariant mass, μ is the signal yield, B is the number of background events within the window, $\phi(m_{e^+e^-}|m_{A'}, \sigma_{m_{A'}})$ is a Gaussian probability distribution describing the signal and $p(m_{e^+e^-}|\mathbf{t})$ is a Chebyshev polynomial of the first kind with coefficients $\mathbf{t} = (t_1, ...t_j)$ that is used to describe the background shape. From optimization studies, a 5th (3rd) order Chebyshev polynomial was found to best describe the background below (above) 39 MeV. Note that $m_{A'}$ and $\sigma_{m_{A'}}$ are set to the A' mass hypothesis and expected experimental mass resolution, respectively. Estimating the signal yield, the background normalization, and the background shape parameters within a window is done with a binned maximum likelihood fit using a bin width of .05 MeV, which was found to have the lowest signal bias. A detailed discussion of the procedures followed

can be found in [29]. Briefly, the log of the ratio of likelihoods for the background-only fit to that of the best signal-plus-background fit provides a test statistic from which the p-value can be calculated, giving the probability that the observed signal is a statistical fluctuation. The p-value is corrected for the "Look Elsewhere Effect" (LEE) by performing simulated resonance searches on 4,000 pseudo data sets. This relates the minimum p-value seen in a given mass bin to the global probability of observing that p-value in the search of the entire mass spectrum.

V. RESULTS

A search for a resonance in the e^+e^- invariant mass spectrum, shown in Figure 2, between 19 MeV and 81 MeV found no evidence of an A' signal. The most significant signal was observed at 37.7 MeV and has a local p-value of 0.17%. After accounting for the LEE correction, the most significant p-value is found to have a global p-value of 17% corresponding to less than 2σ in significance. Since no significant signals were found, a 2σ upper limit is set, power-constrained to the expected limit.

The proportionality between A' and radiative trident production allows the normalization of the A' rate to the measured rate of trident production [20]. This leads to a relation that allows the signal upper limit, $S_{\rm up}$, to be

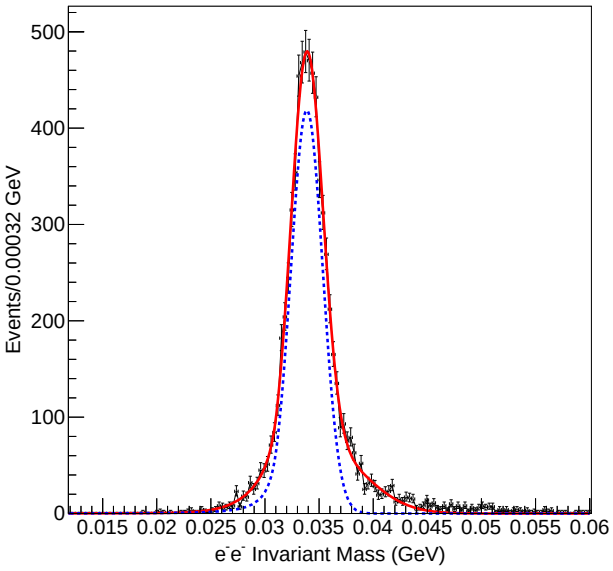

FIG. 1: The Møller mass peak used to measure the mass resolution. The peak was fit with a Crystal Ball function plus a Gaussian for the tail at high mass. The σ of the Crystal Ball function was taken as the mass resolution. The overall fit is in red; the core Crystal Ball in dashed blue.

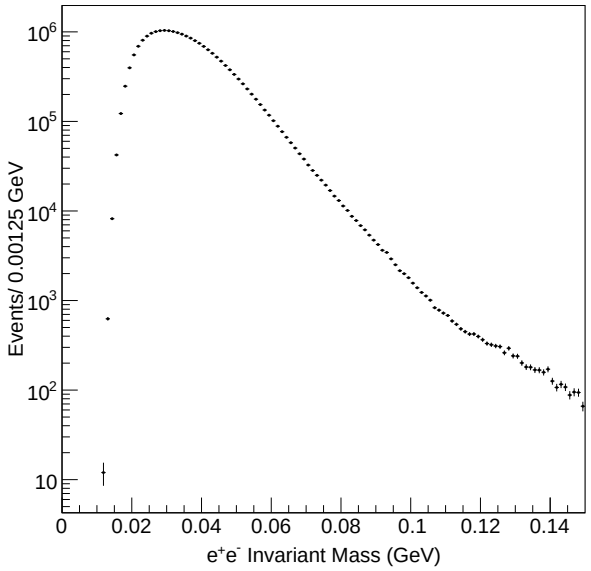

FIG. 2: Distribution of e^+e^- invariant masses, events per 1.25 MeV mass bin vs. mass.

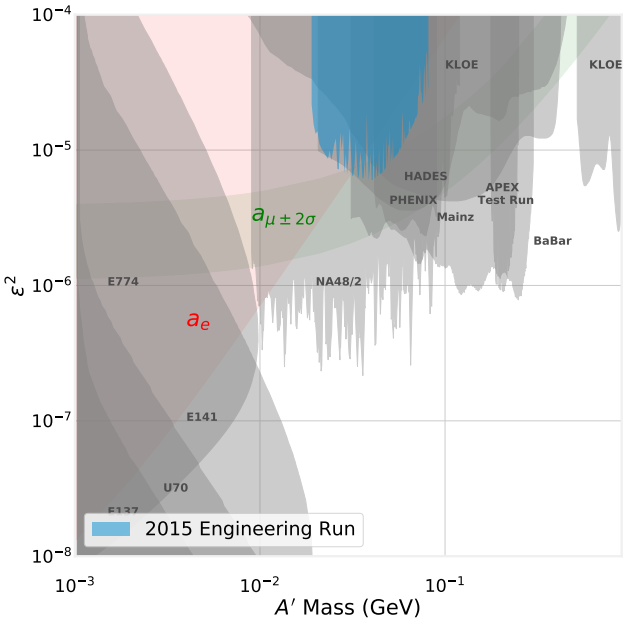

FIG. 3: The 2σ upper limits on ϵ^2 versus A' mass obtained in this analysis. A limit at the level of a 6×10^{-6} is set. Existing limits from other experiments are also shown.

related to the A' coupling strength as

$$\epsilon^2 = \left(\frac{S_{\rm up}/m_{A'}}{f\Delta B/\Delta m}\right)\left(\frac{2N_{eff}\alpha}{3\pi}\right) \qquad (3)$$

where N_{eff} is the number of decay channels kinematically accessible (=1 for HPS searches below the dimuon

threshold), $\Delta B/\Delta m$ is the number of background events per MeV and $f = 8.5\%$ is the fraction of radiative trident events comprising the background. Using equation 3, the limits on ϵ set by HPS are shown on Figure 3.

The reach shown in Figure 3 includes all statistical and systematic uncertainties. The main systematic uncertainty on the signal yields arise from the uncertainty in the mass resolution (3%) and biases observed in the fit due to the background and signal parameterization (1.3-1.5%, depending on mass). The primary systematic when scaling the extracted signal yield upper limits to a limit on epsilon is due to the uncertainty in the radiative fraction due to the unknown composition of the final e^+e^- sample (7%). Many other possible sources of systematic uncertainty were investigated and accounted for but contribute negligibly to the result.

VI. CONCLUSION

A resonance search for a heavy photon with a mass between 19 and 81 MeV which decays to an e^+e^- pair was performed. A search for a resonance in the e^+e^- invariant mass spectrum yielded no significant excess and established upper limits on the square of the coupling at the level of a few times 10^{-6}, confirming results of earlier searches. While not covering new territory in this short engineering run, this search did establish that HPS operates as designed and will, with future running, extend coverage for ϵ^2 below the level of 10^{-6}. Coverage of unexplored parameter space at smaller values of the coupling will be possible from a search for events with displaced vertices.

VII. ACKNOWLEDGMENTS

The authors are grateful for the outstanding efforts of the Jefferson Laboratory Accelerator Division and the Hall B engineering group in support of HPS. The research reported here is supported by the U.S. Department of Energy Office of Science, Office of Nuclear Physics under contract DE-AC05-06OR23177, Office of High Energy Physics under contract DE-AC02-76SF00515, French National Research Agency (ANR-13-JS05-0001), Sesame project HPS@JLab funded by the French region Ile-de-France and the Italian Istituto Nazionale di Fisica Nucleare

[1] J. Hewett, H. Weerts, R. Brock, J. Butler, B. Casey, et al. (2012), 1205.2671.
[2] R. Essig, J. A. Jaros, W. Wester, et al., in *Proceedings, 2013 Community Summer Study on the Future of U.S. Particle Physics: Snowmass on the Mississippi (CSS2013): Minneapolis, MN, USA, July 29-August 6, 2013* (2013), 1311.0029, URL `http://inspirehep.net/record/1263039/files/arXiv:1311.0029.pdf`.
[3] M. Battaglieri et al. (2017), 1707.04591.
[4] J. Jaeckel and A. Ringwald, Ann.Rev.Nucl.Part.Sci. **60**, 405 (2010), 1002.0329.
[5] B. Holdom, Phys.Lett. **B166**, 196 (1986).
[6] P. Galison and A. Manohar, Phys.Lett. **B136**, 279 (1984).
[7] N. Arkani-Hamed and N. Weiner, JHEP **0812**, 104 (2008), 0810.0714.
[8] M. Baumgart, C. Cheung, J. T. Ruderman, L.-T. Wang, and I. Yavin, JHEP **0904**, 014 (2009), 0901.0283.
[9] R. Essig, P. Schuster, and N. Toro, Phys. Rev. **D80**, 015003 (2009), 0903.3941.
[10] N. Arkani-Hamed, D. P. Finkbeiner, T. R. Slatyer, and N. Weiner, Phys.Rev. **D79**, 015014 (2009), 0810.0713.
[11] M. Pospelov and A. Ritz, Phys.Lett. **B671**, 391 (2009), 0810.1502.
[12] D. P. Finkbeiner and N. Weiner, Phys.Rev. **D76**, 083519 (2007), astro-ph/0702587.
[13] P. Fayet, Phys.Rev. **D70**, 023514 (2004), hep-ph/0403226.
[14] M. Kaplinghat, S. Tulin, and H.-B. Yu, Phys. Rev. Lett. **116**, 041302 (2016), 1508.03339.
[15] M. Pospelov, Phys.Rev. **D80**, 095002 (2009), 0811.1030.
[16] G. Bennett et al. (Muon G-2 Collaboration), Phys.Rev. **D73**, 072003 (2006), hep-ex/0602035.
[17] M. Davier, A. Hoecker, B. Malaescu, and Z. Zhang, Eur.Phys.J. **C71**, 1515 (2011), 1010.4180.
[18] C. Cheung, J. T. Ruderman, L.-T. Wang, and I. Yavin (2009), 0902.3246, URL `http://arxiv.org/abs/0902.3246`.
[19] D. E. Morrissey, D. Poland, and K. M. Zurek, JHEP **0907**, 050 (2009), 0904.2567.
[20] J. D. Bjorken, R. Essig, P. Schuster, and N. Toro, Phys. Rev. **D80**, 075018 (2009).
[21] M. Reece and L.-T. Wang, JHEP **07**, 051 (2009).
[22] M. Freytsis, G. Ovanesyan, and J. Thaler, JHEP **1001**, 111 (2010), 0909.2862.
[23] P. H. Adrian et al., Paper in preparation. (2018).
[24] I. Balossino et al. (HPS), Nucl. Instrum. Meth. **A854**, 89 (2017), 1610.04319.
[25] N. Baltzell et al. (HPS), Nucl. Instrum. Meth. **A859**, 69 (2017), 1612.07821.
[26] M. J. French et al., Nucl. Instrum. Meth. **A466**, 359 (2001).
[27] R. Herbst et al., in *Proceedings, 21st Symposium on Room-Temperature Semiconductor X-ray and Gamma-ray Detectors (RTSD 2014): Seattle, WA, USA, November 8-15, 2014* (2016), p. 7431254.
[28] H. Dong et al., Nuclear Science Symposium Conference Record, 2007. NSS '07. IEEE **JLAB-PHY–07-810** (2008).
[29] G. Cowan, K. Cranmer, E. Gross, and O. Vitells, Eur. Phys. J. **C71**, 1554 (2011), [Erratum: Eur. Phys. J.C73,2501(2013)], 1007.1727.